JOURNAL OF MATERIALS SCIENCE **37** (2002) 4555–4559

The pressure-assisted master sintering surface

K. AN*, D. L. JOHNSON†
Department of Materials Science and Engineering, Northwestern University, Evanston, IL 60208-3108, USA
E-mail: dl-johnson@nwu.edu

It has been reported that the master sintering curve (MSC), in which the sintered density is a unique function of the integral of a temperature function over time, is insensitive to the heating path. The present research was undertaken to determine whether the MSC concept is applicable to hot pressing, and to develop the pressure-assisted master sintering surface for alumina. Densification of Sumitomo AKP30 alumina was continuously recorded during heating at 10°C/min at fixed pressures from 7 to 34.5 MPa. Final densities computed from the dilatometer traces were in excellent agreement with values determined by the Archimedes method. The thermocouple was calibrated using the melting point of the Ni/C eutectic. An accuracy of ±2°C was established. The pressure-assisted master sintering surface was successfully constructed. Using this surface, the final density can be predicted to about 1% accuracy for a fixed pressure and an arbitrary temperature-time path.

1. Introduction

Hot pressing is an effective method for a densification of ceramics using thermal and mechanical energy. It can fabricate fully dense, fine-grained ceramic bodies at lower temperatures and at shorter cycle times than those required by conventional sintering techniques [1–3]. The applied pressure induces additional mechanisms which are more complicated than those occurring in normal sintering. Several mechanisms have been proposed to explain the observed enhanced densification during hot pressing.

Vasilos and Spriggs [1] suggested that apparent diffusion coefficients for alumina and magnesia calculated from hot pressing data are orders of magnitude greater than for pressureless sintering, which might be explained by enhanced diffusion under pressure. They found that the consistency in calculated diffusion coefficients as well as a reasonable comparison of activation energies suggests that densification beyond the initial stages is a diffusion-controlled process for the pressures used.

Rahaman *et al.* [4] proposed two densification mechanisms for the reaction hot-pressing of powder compositions near the β'-sialon phase of the Si-Al-O-N system. The mechanisms were interpreted in terms of grain boundary sliding in the presence of a second phase for the composition containing the smallest amount of second phase and a diffusion step of the liquid-phase solution-diffusion-reprecipitation process for the composition containing the largest amount of second phase. In another work, they observed simultaneous creep and densification during sintering of CdO under light uniaxial stresses using a loading dilatometer [5]. They separated the effects of creep and densification. The creep measurements permitted the determination of the sintering strees, which was found to decrease with increasing density when grain growth occurs. They concluded that grain boundary diffusion was the dominant transport mechanism.

While normal stresses across a grain boundary will enhance grain boundary and volume diffusion and therefore sintering [6], several other mechanisms have been described for the observed enhanced densification. These include grain boundary sliding, agglomerate fragmentation, plastic flow, and power law creep [7–11]. Many modeling studies have reported greater or lesser success in describing hot pressing and hot isostatic pressing [12–17].

As an alternative to mechanistic modeling, Su and Johnson developed the concept of the master sintering curve (MSC) for pressureless sintering [18]. The MSC characterizes the sintering behavior for a given powder regardless of the heating history. The MSC was derived from a combined stage sintering model which includes both volume and grain-boundary diffusion mechanisms [19, 20]. The instantaneous densification rate in the latter model is

$$\frac{\mathrm{d}\rho}{\rho \mathrm{d}t} = \frac{3\gamma\Omega}{kT}\left(\frac{\Gamma_{\mathrm{v}} D_{\mathrm{v}}}{G^3} + \frac{\Gamma_{\mathrm{b}}\delta D_{\mathrm{b}}}{G^4}\right) \qquad (1)$$

where γ is the surface energy, Ω the atomic volume, k the Boltzmann constant, T the absolute temperature, G the mean grain diameter, D_{v} and D_{b} the coefficients

* *Present Address*: Pohang Iron & Steel Co., Pohang, Gyungbuk, South Korea.
† Author to whom all correspondence should be addressed.

of volume and grain boundary diffusions, respectively and δ the width of the grain boundary. Γ_v and Γ_b are (non-constant) lumped scaling parameters that relate various geometric features, the driving force for sintering, and the mean diffusion distance to the grain size.

This equation can be rearranged for either grain boundary or volume diffusion such that all terms that are not explicitly functions of temperature are carried to the left hand side, and then integrated, as follows:

$$\frac{k}{\gamma \Omega D_o} \int_{\rho_o}^{\rho} \frac{G^n}{3\rho\Gamma} \, d\rho = \int_0^t \frac{1}{T} \exp\left(-\frac{Q}{RT}\right) dt \quad (2)$$

where Q is the apparent activation energy, D_o is the pre-exponential term for the diffusion coefficient, (including δ in the case of grain boundary diffusion), R is the gas constant, and $n = 3$ or 4 for volume or grain boundary diffusion, respectively.

A mechanistic model would attempt to integrate both sides of this equation. For the master sintering curve, the measured density is plotted as a function of the right hand side, hereafter denoted Θ. If a single mechanism is responsible for densification, the sintered density can be predicted from the curve irrespective of the heating path.

The motivation for the present study was to determine whether the concept of the master sintering curve can be extended into the realm of hot pressing, and to establish the pressure-assisted master sintering surface (PMSS) of an alumina powder.

2. Experimental procedures

A schematic cross section of the hot press die assembly and furnace[1] is illustrated in Fig. 1. Pressure is applied by a single acting ram from the bottom, but double action results since the die can move freely upward as pressure is applied. The die assembly is enclosed by the graphite heating element which is completely surrounded by graphite felt insulation. A Type C thermocouple with a 3 mm diameter Nb/1% Zr sheath[2] was inserted in the side of the die to about 6 mm from the specimen. The chamber was evacuated by a mechanical pump to 500 mtorr and then backfilled with high purity Ar gass (99.998%). The pressure of Ar gas was maintained between 20 and 35 kPa.

A dilatometer was installed to determine the linear shrinkage from the relative motion of the pressing ram with respect to the water-cooled bottom plate of the furnace. The pressure was measured electronically.[3] An A/D converter and computer acquired linear shrinkage, temperature and pressure data continuously.

The temperature measurement system was calibrated using pressed compacts of pure Ni powder[4] and Ni powder mixed with 2.1 wt% C, the eutectic composition. Pellets 19 mm in diameter and 1.4 mm thick were placed in the 25.4 mm diameter die chamber and

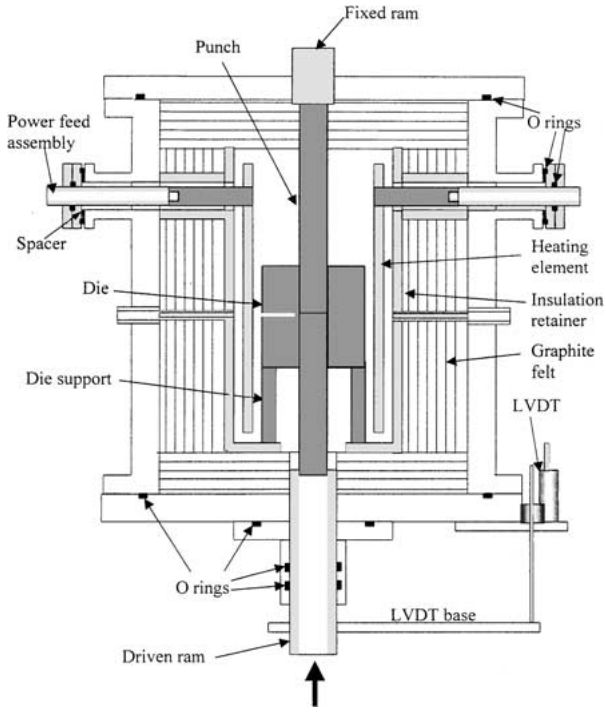

Figure 1 Schematic diagram of the hot press.

separated from the punches by graphite foil. A pressure of 1.4 MPa was applied at room temperature and maintained during heating at 10°/min to 1500°C. The temperature at which an abrupt change in shrinkage occurred was taken as the onset of melting at the eutectic temperature.

For hot pressing, α-Al_2O_3 powder (99.99% purity, AKP-30, Sumitomo) having an average particle diameter of 0.4 μm was mixed with 3 wt% of polyvinyl butyral binder in acetone, dried, granulated, and screened to -60 mesh. Pellets 25.4 mm in diameter by $\sim$2 mm thick were pressed at 300 MPa and the binder was burned out at 650° in air. This resulted in negligible densification but provided green strength and minimized contamination from any adsorbed species in the raw powder.

Three different heating and pressure schedules were used. First, 20.7 MPa pressure was applied at room temperature and then the furnace was heated at 10°/min in separate runs to 1100°, 1200°, 1300°, or 1400°, followed by a 30 minute hold at the indicated temperature. An additional specimen was heated at 13°/min to 1832° and held for 30 minutes.

Secondly, hot pressing using applied pressures from 6.9 to 34.5 MPa were conducted. Pressure was applied at room temperature and a constant heating rate of 10°/min was maintained from room temperature to 1500° without an isothermal hold.

Finally, the runs for pressureless sintering were carried out in the same system by heating at 10°/min to 1400° and then held isothermally for 0, 30 and 60 minutes.

Microstructures were examined by scanning electron microscopy on fracture surfaces. Bulk and apparent densities as well as open and closed porosity levels were determined by the Archimedes method. For this measurement, specimens were immersed in water,

[1] Centorr Associates, Inc., Suncook, NH.

[2] ARi Industries (UK) Ltd., Camberley, Surry, UK.

[3] Model 204, Setra Systems, Acton, MA.

[4] Mond 255, INCO Limited, Toronto, Canada.

boiled for 30 minutes and cooled to room temperature before determining the submerged and saturated masses.

3. Results and discussion

Fig. 2 shows the dilatometer data for the temperature calibration. The break in the slopes occurs when the eutectic temperature is reached and the Ni begins to react with C to produce eutectic liquid. The vertical broken line is at the published eutectic temperature. 1318° [21]. Linear regression line fits to the segments above and below the breaks in the curves intersected at 1320° for Ni powder and 1317° for the Ni/2.1% C. These results indicate that the temperature was known at an accuracy of about ±2° at this temperature. It was assumed that the accuracy over the temperature range of interest was not greatly different from this.

It was necessary to calibrate the dilatometer to account for thermal expansion of the system. To do this, trial runs without pellets were made under identical pressure and temperature conditions that would be employed for the specimens. The net shrinkage of the specimens was determined from the difference between the blank and specimen runs. Linear shrinkage was converted to densification beginning with the final Archimedes bulk density and working backward in time.

A test of the applicability of the master sintering curve to hot pressing was made by comparing the densities of the specimens hot pressed at 20.7 MPa with 30 minute holds at 1100° to 1400° with the density computed from the dilatometer trace during constant heating rate to 1500° at the same pressure and heating rate. The density as a function of temperature is shown in Fig. 3. Here the density of the specimens held at temperature would follow the dilatometer trace to the holding temperature and then climb to the final value during the 30 minute hold. When the density is plotted as a function of log(Θ), where Θ is defined as the integral of the right hand side of Equation 2, the two data sets merge onto a single curve, which is a constant pressure trace on the pressure-assisted master sintering surface (Fig. 4). An activation energy of 477 kJ/mol was assumed, which is the value used by Frost and Ashby [22]. The agreement is excellent, indicating that the master sintering curve concept can be applied to hot pressing.

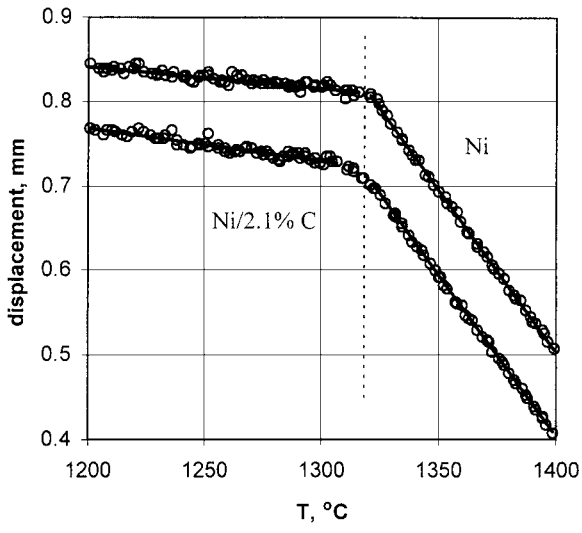

Figure 2 Dilatometer data for powder Ni and Ni/2.1% C compacts during heating at 10°/min.

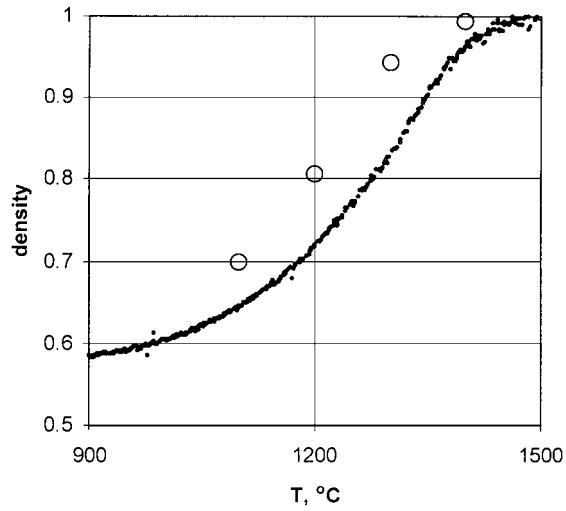

Figure 3 Density as a function of hot pressing temperature at 20.7 MPa. Large circles: Archimedes density of individual specimens heated at 10°/min to various temperatures and held 30 minutes. Small circles: dilatometer data for a single specimen heated at 10°/min to 1500° with no hold.

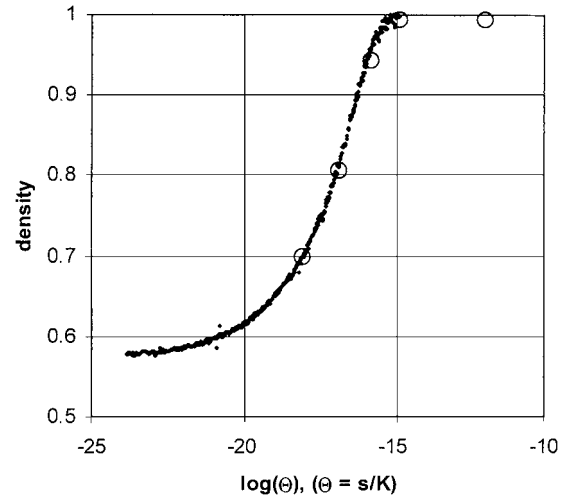

Figure 4 Master sintering curve for data of Fig. 3.

The density as a function of temperature for a heating rate of 10°C/min using constant applied pressures of from 6.9 to 34.5 MPa is given in Fig. 5. Fig. 6 shows the constant pressure contours of the pressure-assisted master sintering surface constructed from the densification data displayed in Fig. 5, as well as that of the pressureless-sintered specimens determined by the Archimedes method. To develop other views, points were picked at 0.65, 0.70, . . . 0.95 for each of the constant pressure curves and multiple regression analysis was done to obtain an empirical model of the PMSS. The resulting surface is shown in Fig. 7. Fig. 8 shows a constant density contour plot of the PMSS, along with the data points from which it was obtained, projected onto the pressure-log(Θ) plane. The view down the log(Θ) axis is shown in Fig. 9.

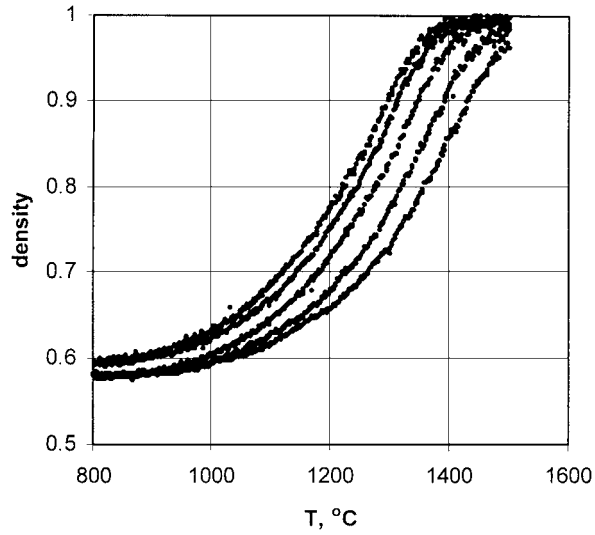

Figure 5 Relative density versus temperature using a constant heating rate of 10°/min at varying applied pressure from 6.9 to 34.5 MPa. Pressures are, from right to left, 6.9, 13.8, 20.7, 27.6, and 34.5 MPa.

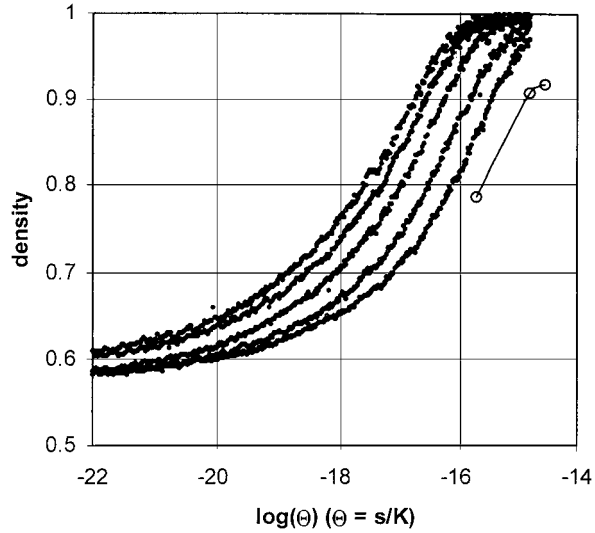

Figure 6 Constant pressure contours of the pressure-assisted master sintering surface (PMSS) of Sumitomo AKP30 alumina constructed using the data of Fig. 5. Pressures are, from right to left, 0, 6.9, 13.8, 20.7, 27.6, and 34.5 MPa.

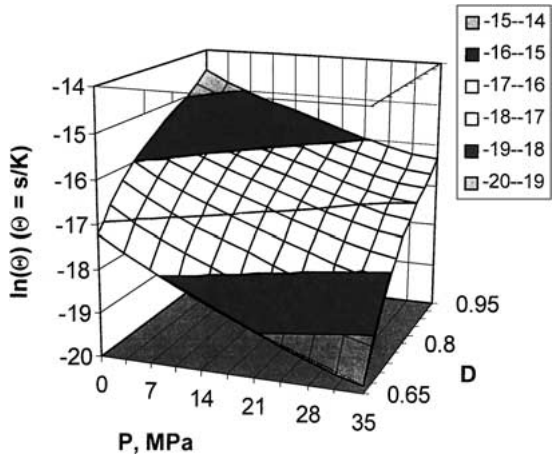

Figure 7 Perspective view of the PMSS.

Having determined the PMSS, it now is possible to predict the density of a specimen hot pressed at any pressure from 0 and 34.5 MPa if the temperature-time trajectory is known. Conversely, one can specify the time-temperature excursion at any pressure in this range to achieve a given density. For instance, Table I shows a variety of conditions that would yield compacts of 95% dense hot pressed at 34.5 MPa.

TABLE I Predicted hot pressing conditions to yield compacts of 95% density at 34.5 MPa ($\Theta = 4.8 \cdot 10^{-17}$ s/K)

Heating rate (°C/min)	Cooling rate (°C/min)	Hold time	Peak T (°C)
10	10	0	1302
10	50	0	1323
10	10	20	1250
20	20	0	1331
50	50	0	1373

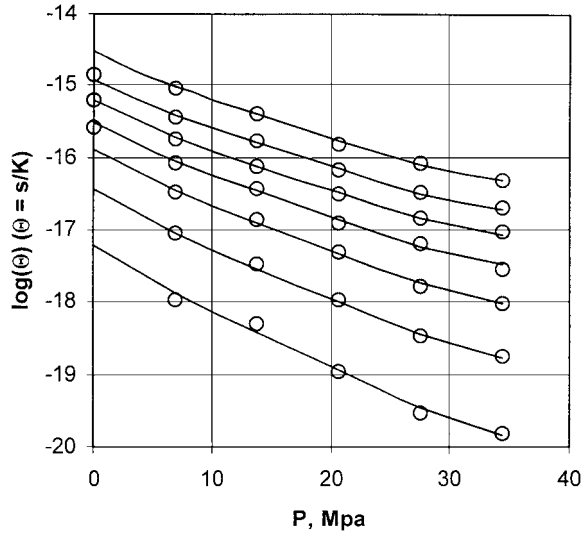

Figure 8 Constant density contours of the PMSS. Contours are, from bottom to top, 0.65 to 0.95 in increments of 0.05.

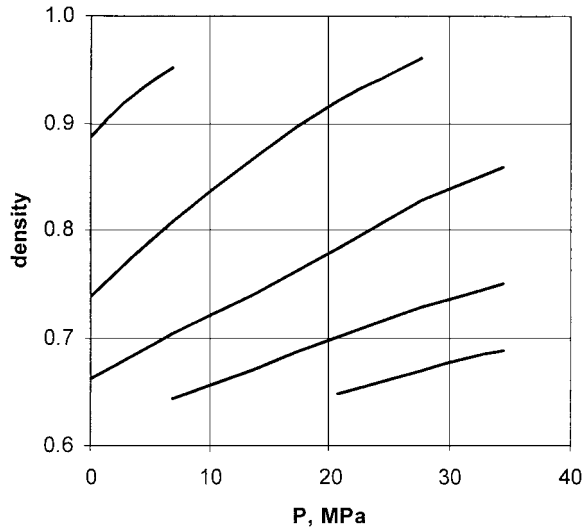

Figure 9 Constant log(Θ) contours of the PMSS. Contours are, from upper left to lower right, −15, −16,. . ., −19 s/K.

4. Conclusions

A trial of the application of the master sintering curve to hot pressing was made to see whether a unique densification curve exists under a pressure of 20.7 MPa. The density continuously determined by the dilatometer plotted versus the integral of a temperature function

over time, Θ, agreed well with the densities determined by the Archimedes method after hot pressing at the same pressure but with a different heating history. Thus the density versus Θ profile can be used to predict the final density at a given pressure regardless of heating history. The study was extended to a range of pressures from 0 to 34.5 MPa to generate the pressure-assisted master sintering surface. This surface enables the prediction of the final density at a fixed pressure and an arbitrary heating history. It also can be used to specify the heating schedule required to achieve a desired density at a given pressure.

Acknowledgment

This work was performed under the support of the U.S. Department of Commerce, National Institute of Standards and Technology, Advanced Technology Program, Cooperative Agreement 70NANB7H3020.

References

1. T. VASILOS and R. M. SPRIGGS, *J. Amer. Ceram. Soc.* **46** (1963) 493.
2. P. H. CRAYTON and J. J. PRICE, *Ceramic Bulletin* **63** (1984) 715.
3. G. J. LESHKIVICH and P. H. CRAYTON, *Am. Ceram. Soc. Bull.* **64** (1985) 684.
4. M. N. RAHAMAN, F. L. RILEY and R. J. BROOK, *J. Amer. Ceram. Soc.* **63** (1980) 648.
5. M. N. RAHAMAN, L. C. DE JONGHE and R. J. BROOK, *ibid.* **69** (1986) 53.
6. D. LYNN JOHNSON, *Scripta Met.* **3** (1969) 567.
7. R. L. COBLE and J. S. ELLIS, *J. Amer. Ceram. Soc.* **46** (1963) 438.
8. G. E. GAZZA, "Engineering Metal Handbook, Ceramics and Glasses," Vol. 4 (ASM International, Metal Park, OH, 1991) p. 296.
9. R. L. COBLE, *J. Appl. Phys.* **41** (1970) 4798.
10. M. R. NOTIS and P. WINGERT, *Science of Sintering* **10** (1978) 35–44.
11. H. S. KIM and D. N. LEE, *Mater. Sci. Eng. A-Struct. Mater.* **271** (1999) 424.
12. P. MURRAY, D. T. LIVEY and J. WILLIAMS, "Ceramic Fabrication Processes," edited by W. D. Kingery (Technology Press of Massachusetts Institute of Technology and John Wiley & Sons, NY, 1958) p. 147.
13. J. D. McCLELLAND, *J. Amer. Ceram. Soc.* **44** (1961) 526.
14. R. M. SPRIGGS and T. VASILOS, *ibid.* **47** (1964) 47.
15. R. C. ROSSI and R. M. FULRATH, *ibid.* **48** (1965) 558.
16. P. L. FARNSWORTH and R. L. COBLE, *ibid.* **49** (1966) 264.
17. L. T. KUHN, R. M. McMEEKING and F. F. LANGE, *ibid.* **74** (1991) 682.
18. H. SU and D. L. JOHNSON, *ibid.* **79** (1996) 3211.
19. J. D. HANSEN, R. P. RUSIN, M. TENG and D. L. JOHNSON, *ibid.* **75** (1992) 1129.
20. D. L. JOHNSON, R. P. RUSIN and J. D. HANSEN, in "Sintering-Advances in Powder Metallurgy and Particulate Materials," Vol. 3 (Metal Powder Industries Foundation, Princeton, NJ, 1992) p. 17.
21. E. A. BRANDES, in "Metals Reference Book," 6th ed. (Butterworth, London, 1983) p. 11.
22. H. J. FROST and M. F. ASHBY, "Deformation-Mechanism Maps: The Plasticity and Creep of Metals and Ceramics" (Pergamnon Press, Oxford, 1982).

Received 9 January
and accepted 3 July 2002